

Simple models of cooling flows

James Binney¹ & Christian Kaiser²

¹Theoretical Physics, 1 Keble Road, Oxford OX1 3NP

²Department of Physics & Astronomy, University of Southampton, Southampton, SO17 1BJ

arXiv:astro-ph/0207111v1 4 Jul 2002

Received ...; accepted ...

ABSTRACT

A semi-analytic model of cluster cooling flows is presented. The model assumes that episodic nuclear activity followed by radiative cooling without mass-dropout cycles the cluster gas between a relatively homogeneous, nearly isothermal post-outburst state and a cuspy configuration in which a cooling catastrophe initiates the next nuclear outburst. Fitting the model to *Chandra* data for the Hydra cluster, a lower limit of 284 Myr until the next outburst of Hydra A is derived. Density, temperature and emission-measure profiles at several times prior to the cooling catastrophe are presented. It proves possible to fit the mass $M(\sigma)$ with entropy index $P\rho^{-\gamma}$ less than σ to a simple power-law form, which is almost invariant as the cluster cools. To high precision, the central value of σ decreases linearly in time. The fraction of clusters in a magnitude-limited sample that have gas cooler than T is calculated, and is shown to be small for $T = 2$ keV. Similarly, only 1 percent of clusters in such a sample contain gas with $P\rho^{-\gamma} < 2$ keV cm². Entropy production in shocks is shown to be small. The entropy that is radiated from the cluster can be replaced if a few percent of the cluster gas passes through bubbles heated during an outburst of the AGN.

Key words: cooling flows – galaxies: clusters – galaxies: clusters: individual: Abell 780 – galaxies: active

1 INTRODUCTION

Observations from the *Chandra* and *XMM-Newton* missions have shown that the intergalactic medium of cooling-flow clusters is not a multiphase medium of the type required by the theory of cooling flows that has been widely accepted for over a decade (e.g. Fabian 1994). Moreover, when these data are taken together with earlier radio and optical data, it is now clear that over the lifetimes of these systems very little gas has cooled to temperatures much below the virial temperature. Consequently, these systems cannot be the scenes of a quiescent steady inflow regulated by distributed ‘mass dropout’ as that theory postulated. In the light of the new observations, increasing numbers of workers (e.g. Böhringer et al. 2002, and references therein) are accepting the view that catastrophic cooling of intergalactic gas to very low temperatures takes place only at very small radii, and that on larger scales the intergalactic medium is periodically reheated by an active galactic nucleus (AGN) that is fed by central mass dropout. This general picture has been argued for several times over the last decade (Tabor & Binney 1993; Binney & Tabor 1995; Binney 1996, 1999; Ciotti & Ostriker 1997; Binney 2002), but the physics involved is complex because the problem is inherently three-dimensional and un-

steady, and many details remain to be filled in now that clearer observations are becoming available.

Although the mechanism by which the AGN heats the IGM is unclear – possibilities include the impact on ambient thermal plasma of collimated outflows from the AGN (Heinz et al. 1998; Kaiser & Alexander 1999; Binney 1999) and inverse Compton scattering by thermal plasma of hard photons from the AGN (Ciotti & Ostriker 1997, 2001) – features have been observed near the centres of several clusters that are almost certainly bubbles of hot, low-density plasma that have been created by the AGN. Simulations (Churazov et al. 2001; Saxton et al. 2001; Brüggen & Kaiser 2001; Quilis et al. 2001; Brüggen et al. 2002) suggest that these rise through the cluster’s gravitational potential well on a dynamical timescale. The details of how a rising bubble mixes with surrounding gas and disperses its energy around the intracluster medium cannot be securely deduced from simulations, because they depend on what happens on very small scales at the edge of a bubble. The general idea that heating by AGN results in a kind of convection in the ICM is probably correct, however. The purpose of this note is to present a simple semi-analytical model of the life-cycle of a typical cluster that this process drives.

Section 2 defines the model, fits its initial condition to *Chandra* data for the Hydra cluster, and shows its observ-

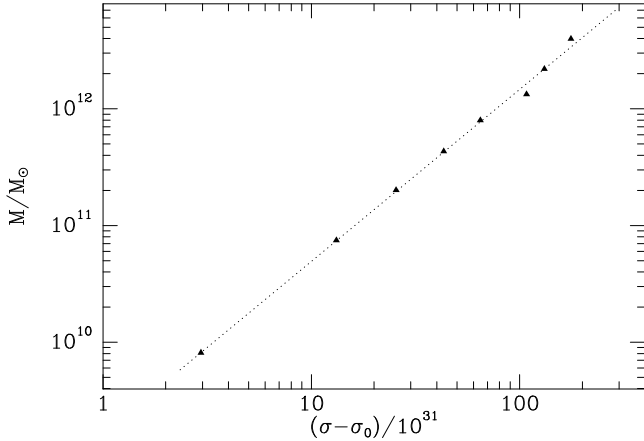


Figure 1. The function $M(\sigma)$ for the Hydra cluster estimated from the data of David et al. (2001). The units of σ are $10^{31} \text{ cm}^4 \text{ g}^{-2/3} \text{ s}^{-2}$ and in these units $\sigma_0 = 17$. The dotted line shows equation (1) with $\epsilon = 1.48$.

able characteristics at a number of later epochs. Section 3 discusses the creation of entropy during an outburst of the AGN and estimates the fraction of the cluster gas that an outburst processes through bubbles. Section 4 calculates the distribution of cluster-centre temperatures in a magnitude-limited sample of clusters and shows that temperatures below $\sim 2 \text{ keV}$ will very rarely be detected. Section 5 similarly calculates the distribution of the minimum values of the specific entropy that will be detected in a survey. Section 6 sums up. Throughout we assume a flat cosmology with $\Omega_\Lambda = 0.7$ and $H_0 = 65 \text{ km s}^{-1} \text{ Mpc}^{-1}$.

2 THE MODEL

Gas that is in stable hydrostatic equilibrium is stratified by specific entropy s , such that s never decreases as one moves up the gravitational potential. Heating by an AGN disturbs this equilibrium by producing bubbles of high-entropy gas near the bottom of the well. On a dynamical timescale each bubble rises through the well, shedding as it goes gas of the appropriate value of s to each isopotential shell. Following this rearrangement, the gas is in approximate hydrostatic equilibrium, but slowly radiates entropy. After a finite time, the gas at the bottom of the well, which initially has the least entropy and the highest density, has radiated all its entropy. Its density is then extremely large and a further outburst of the AGN is stimulated when some of this dense gas accretes onto the central massive black hole. This new outburst starts the next cycle of the system.

If P denotes pressure, ρ gas density and γ the ratio of the principal specific heats, then $s = \text{constant} + \frac{3}{2}k_B \ln(\sigma)$, where $\sigma \equiv P\rho^{-\gamma}$ will be called the ‘entropy index’ and k_B is the Boltzmann constant. Let $M(\sigma)$ be the gas mass with entropy index less than σ ; Fig. 1 shows an estimate of $M(\sigma)$ for the Hydra cluster from the data of (David et al. 2001, hereafter D2001) plotted such that a straight line corresponds to the functional form

$$M(\sigma) = A(\sigma - \sigma_0)^\epsilon. \quad (1)$$

Since the data fall near a line, we assume that, at least dur-

ing some phases in the evolution of the cluster gas, $M(\sigma)$ can be adequately fitted by this functional form. The fit involves three free parameters, A , ϵ and σ_0 . The lowest entropy density index found in the cluster gas is σ_0 at the cluster centre. It is therefore intimately related to the time that must elapse before the next outburst of the AGN. The total mass of the cluster gas is given by

$$M_{\text{tot}} = A(\sigma_{\text{max}} - \sigma_0)^\epsilon, \quad (2)$$

where σ_{max} is the highest entropy index of the cluster gas at the largest radius. This relation defines the constant A .

Given a functional form $M(\sigma)$ one can find the hydrostatic equilibrium configuration of the gas in a given spherical gravitational potential $\Phi(r)$ as follows. Eliminating ρ from the equation of hydrostatic equilibrium we have

$$\frac{dP}{dr} = - \left(\frac{P}{\sigma} \right)^{1/\gamma} \frac{d\Phi}{dr}. \quad (3)$$

A second equation relating P and M is

$$\frac{dM}{dr} = 4\pi r^2 \rho = 4\pi r^2 \left(\frac{P}{\sigma} \right)^{1/\gamma}. \quad (4)$$

For a given $\Phi(r)$ we obtain a model atmosphere by solving the coupled differential equations (3) and (4) from $r = 0$ with the initial conditions $M(0) = 0$ and $P(0) = P_0$, where P_0 is a trial value. At some radius R_{out} the gas mass reaches the value M_{tot} . The central pressure P_0 is adjusted until the pressure at R_{out} is equal to a specified value P_∞ .

It is instructive to recast equation (3) in terms of the gas temperature, T . Assuming the cluster gas to be ideal, we can eliminate P from equation (3) and find

$$\gamma \frac{d \ln T}{dr} = \frac{d \ln \sigma}{dr} - (\gamma - 1) \frac{\mu m_p}{k_B T} \frac{d \Phi}{dr}, \quad (5)$$

where μ is the mean molecular weight. Since the second term on the right side of this equation is intrinsically positive, the indications from observations that $dT/dr > 0$ at most radii requires $d \ln \sigma/dr$ to be significantly greater than zero. Now

$$\frac{d \ln \sigma}{dr} = \frac{d \ln \sigma}{dM} \rho r^2, \quad (6)$$

so $d \ln T/dr$ can be positive near the centre only if $dM/d \ln \sigma$ vanishes rapidly as $M \rightarrow 0$. For our initial assumption for $M(\sigma)$, equation (1), this requirement translates into a lower limit on the exponent ϵ .

2.1 Comparison with Hydra cluster

In this section we calculate model atmospheres for the gas in galaxy clusters. We adjust the model parameters to provide a fit to the density and temperature distributions of the Hydra cluster as inferred from X-ray observations (D2001). We do not attempt a formal fit of the data as this would require folding our model results with the telescope response. We are only interested in a rough constraint on our model parameters to find reasonable values. Thus varying the model parameters and fitting by eye is sufficient. From Fig. 1 we find that for the Hydra cluster $\epsilon \sim 1.5$ in equation (1) and $\sigma_0 = 17 \times 10^{31} \text{ cm}^4 \text{ g}^{-2/3} \text{ s}^{-2}$. Out to the limit of the data at $R_{\text{out}} \sim 230 \text{ kpc}$, the ratio $\sigma_{\text{max}}/\sigma_0 \sim 13.5$. We assume that the gravitational potential has the form of the potential of an NFW dark-matter halo (Navarro et al. 1996). Then there

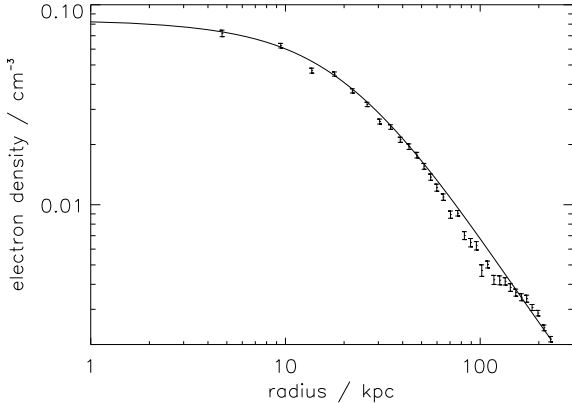


Figure 2. The fit between the unevolved model (curve) and the density in the Hydra cluster inferred from X-ray observations. Data points and errors from D2001.

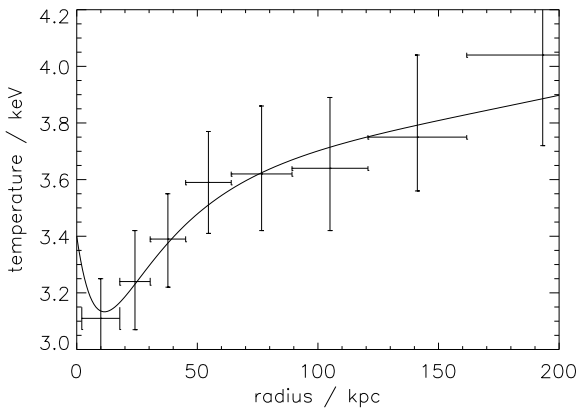


Figure 3. Comparison of the initial model with temperature of the gas in the Hydra cluster inferred from X-ray observations. Data points show the temperatures derived by David et al. (2001). Vertical error bars are the 90% confidence limits and horizontal bars indicate the region within the cluster over which the temperature was averaged. The solid line shows the model.

are four free parameters to determine by fitting the observational data: the gas pressure at the centre of the cluster, P_0 , the gas pressure at R_{out} , P_∞ , the scale length of the NFW profile, r_s , and the overdensity of the dark matter halo compared to the critical density at the redshift of the cluster, δ_c .

Figs 2 and 3 show comparisons of the model with the data. The good fit is achieved for $P_0 = 8.8 \times 10^{-10} \text{ erg cm}^{-3}$ and $P_\infty = 2.6 \times 10^{-11} \text{ erg cm}^{-3}$. The length scale of the NFW profile is $r_s = 79.3 \text{ kpc}$ and the overdensity of the dark matter halo $\delta_c = 8.5 \times 10^4$ for our chosen cosmology. Both values are consistent with the findings of D2001. From these parameters we find the gas density in the cluster centre is $\rho_0 = 1.7 \times 10^{-25} \text{ g cm}^{-3}$, which corresponds to an electron density of 0.085 cm^{-3} . The gas temperature at the centre is $k_B T_0 = 3.4 \text{ keV}$. The mass enclosed within $R_{\text{out}} = 230 \text{ kpc}$ is $M_{\text{tot}} = 5.8 \times 10^{12} h^{-1} M_\odot$.

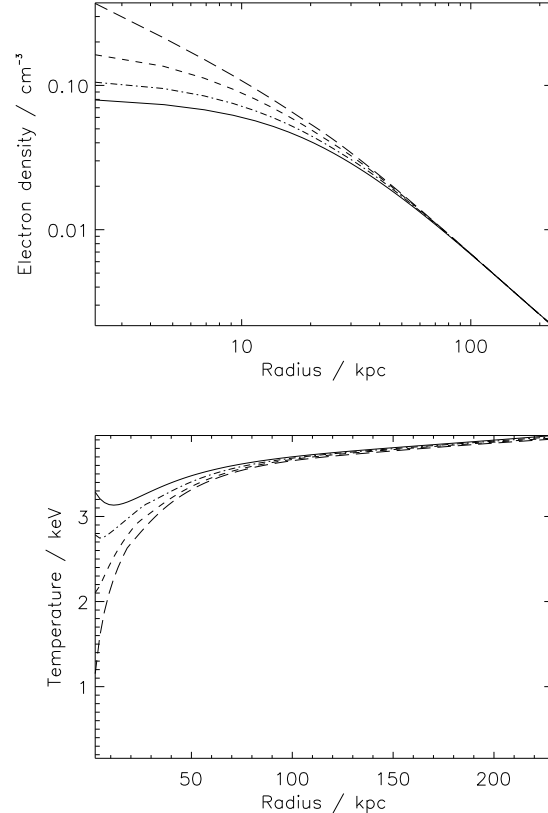


Figure 4. Density and temperature profiles for the Hydra cluster at the present time (full curves), after 100 Myr (dot-dashed curves), 200 Myr (short-dashed curves), and 284 Myr (long-dashed curves).

2.2 Cooling

If $\Lambda(T)$ is the usual cooling function, the rate at which specific entropy is radiated is

$$\dot{s}(r, t) = \frac{3}{2} k_B \frac{\dot{\sigma}}{\sigma} = -\frac{\Lambda(T)}{T} n, \quad (7)$$

where the electron density is

$$n_e(r) = 0.85 \frac{\rho(r)}{m_p}. \quad (8)$$

From Fig. 9-9 of Binney & Tremaine (1987) we calculate the cooling function $\Lambda(T)$ appropriate to metallicity $Z = 0.4 Z_\odot$ (D2001). Then by integrating equation (7) at each value of r for a small time interval δt , we can update the function $\sigma(M)$ that is initially specified by equation (1)

$$\sigma(M) \rightarrow \sigma - \frac{2}{3} \sigma n \frac{\Lambda(T)}{k_B T} \delta t, \quad (9)$$

where the quantities are evaluated at the radius that at time t contains mass M . Assuming $P_\infty = \text{const.}$, we then use equations (3) and (4) to reconstruct the density profile at time $t + \delta t$, and so on. Note that R_{out} will decrease as the cluster gas radiates energy, and the material outside R_{out} slightly compresses the cluster. Fig. 4 shows the resulting predictions for the evolution of the density and temperature profiles of the Hydra cluster.

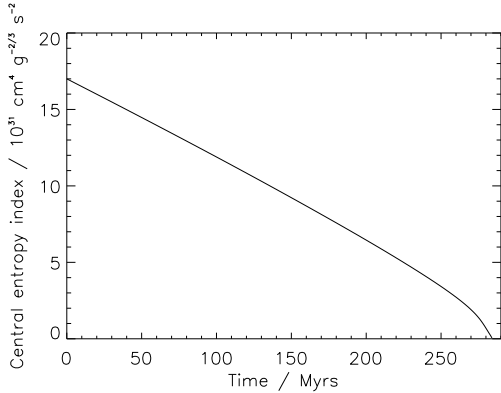


Figure 5. The time-evolution of the central entropy index σ_0 .

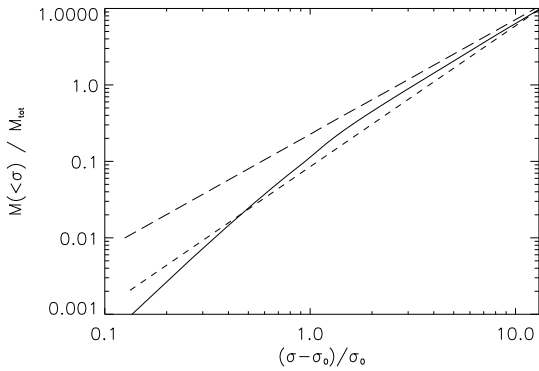


Figure 6. Cumulative mass of the cluster gas as a function of the entropy index. The long-dashed line shows the initial power-law of equation (1). The solid line shows $M(\sigma)$ at $t = 284$ Myr. The short-dashed line represents the power-law giving the best fit to the solid line.

The value of the central temperature halves, and the central density doubles in roughly 240 Myr. The central temperature then drops rapidly to zero in the following 44 Myr. We assume that at this time the central AGN erupts and restores the density and temperature profiles to distributions similar to those currently measured.

Fig. 5 shows the time-evolution of the central entropy index σ_0 . To a very good approximation, it falls linearly in time between $t = 0$ and $t = 260$ Myr. For temperatures above about 2.6 keV our cooling function is dominated by bremsstrahlung, i.e. $\Lambda(T) \propto \sqrt{T}$. In this regime equation (7) implies

$$\dot{\sigma}_0 \propto P_0^{2/5} \sigma_0^{1/10}. \quad (10)$$

The very weak dependence of $\dot{\sigma}_0$ on either P_0 or σ_0 leads to the very nearly linear time dependence of σ_0 . Even for temperatures below 2.6 keV, $\Lambda(T)$ and therefore $\dot{\sigma}_0$ are not strong functions of temperature, so the approximately linear time-evolution of σ_0 holds at nearly all times. Of course, equation (10) also holds for material further out in the cluster. A linear relation between t and σ can thus be used for an accurate estimate of the time to elapse before the next nuclear eruption.

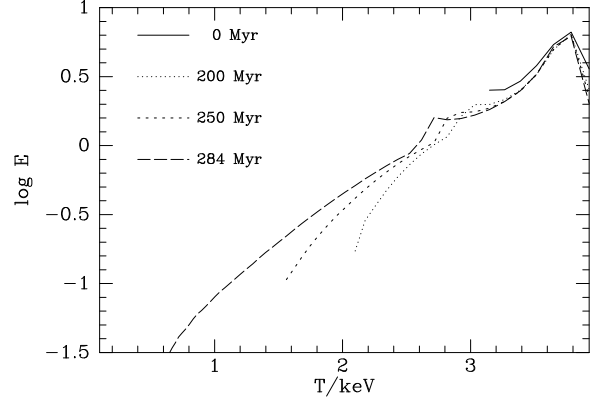


Figure 7. The emission measure of the cluster gas at four different times.

Figure 6 shows the cumulative mass of the cluster gas as a function of σ . Only at times later than about 230 Myr is there a significant deviation from the power-law form of equation (1). In fact, even at $t = 284$ Myr a power-law with exponent $\epsilon = 1.8$ approximates $M(< \sigma)$ to within a factor 2. For gas with an entropy index greater than $2\sigma_0$ a power-law provides an excellent fit throughout the cluster evolution.

The emission measure distribution is defined to be

$$E(t, T) = \int dV \delta(T' - T) n_e^2, \quad (11)$$

where T' is the temperature of the gas in the volume element dV . Figure 7 shows the run of E with T at four times. The evolution of $E(t, T)$ is dominated by the growth of a tail towards low T due to radiative cooling. Gas at $T < 1$ keV appears only at the very end of the evolution. Even gas with $T < 2$ keV appears only at times later than about 245 Myr. We will show in Section 4 that this result explains the lack of observations of very cold gas in galaxy clusters (e.g. Böhringer et al. 2002). The secondary peak at temperatures below the main peak is caused by the break in the density distribution at around 30 kpc (see Figure 4).

3 THE CREATION AND LOSS OF ENTROPY

We now estimate the rate at which the AGN creates entropy in the ICM and compare it with the rate at which entropy is radiated by the ICM. We idealize the blowing of a bubble as a process in which N_1 particles of the ICM are irreversibly heated to a high temperature T_1 from the temperature T_3 at the base of the cooling flow. The heated bubble expands as it is heated and does work on its environment. The interface between the bubble and the ambient medium is Rayleigh-Taylor unstable so it will dissolve on a dynamical time. From the sharpness of the edges of observed bubbles it thus follows that they inflate supersonically. Since material just outside bubbles appears not to be on a high adiabat (Fabian et al. 2000), we infer that the expansion is only mildly supersonic. The entropy generation by weak shocks is small (see appendix), and we neglect it.

The entropy of a non-degenerate ideal monatomic gas of N particles that occupies volume V at temperature T is

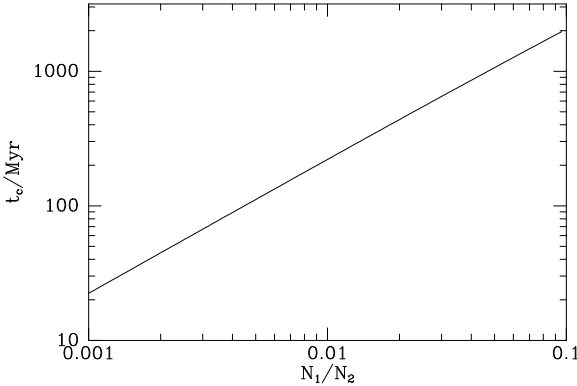


Figure 8. Time t_{cool} required to radiate entropy generated by processing a mass fraction N_1/N_2 of the cluster plasma through bubbles heated to 10 times the ambient temperature.

$$S = Nk_B \left\{ \frac{5}{2} + \ln \left[\frac{V}{N} \left(\frac{2\pi m k_B T}{h^2} \right)^{3/2} \right] \right\}. \quad (12)$$

Hence, when a bubble containing N_1 particles is heated at constant pressure from T_3 to T_1 , the entropy created is

$$S_{\text{infl}} = \frac{5}{2} N_1 k_B \ln(T_1/T_3). \quad (13)$$

Additional entropy is created as the bubble rises and mixes in with the ambient medium. Since most of the cluster gas falls within quite a small range in temperature, we simplify the equations by supposing that the bubble mixes with material that all has temperature T_2 . Let the bubble mix with material that contains N_2 particles and assume for simplicity that the mixing occurs at constant pressure. Then from eq. (12) it is straightforward to show that the entropy of mixing is

$$S_{\text{mix}} = \frac{1}{2} N_1 k_B \ln \left(\frac{1 + N_2 T_2 / (N_1 T_1)}{1 + N_2 / N_1} \right) + \frac{1}{2} N_2 k_B \ln \left(\frac{1 + N_1 T_1 / (N_2 T_2)}{1 + N_1 / N_2} \right) \quad (14)$$

Adding eqs (13) and (14) we get the total entropy created by a bubble. As an illustrative example, if $T_1 = 10T_2$, $T_3 = T_2/10$ and $N_1 = N_2/10$, then $S_{\text{infl}} = 11.5k_B N_1$ and $S_{\text{mix}} = 2.14k_B N_1$. The relative contribution to the total entropy production from S_{mix} increases with N_2/N_1 ; for example with $T_1 = 10T_2$ again but $N_2 = 100N_1$, S_{infl} is unchanged while $S_{\text{mix}} = 3.2k_B N_1$.

We may estimate the fraction of the plasma that is processed through bubbles during an outburst by finding the time taken for gas of density N_2/V_2 at temperature T_2 to radiate the entropy created in an outburst, where V_2 is the volume of the gas. The rate of entropy radiation is

$$\dot{S} = \frac{\Lambda(T_2)(0.52N_2/V_2)^2 V_2}{T_2}, \quad (15)$$

where 0.52 is the conversion factor between total particle density N_2/V_2 and electron density. The time to radiate the entropy created by a bubble is thus

$$t_c = \frac{S}{\dot{S}} = \frac{N_1}{N_2} \left\{ 5 \ln \left[\frac{T_1}{T_3} \right] + \ln \left[\frac{1 + N_2 T_2 / (N_1 T_1)}{1 + N_2 / N_1} \right] + \frac{N_2}{N_1} \ln \left[\frac{1 + N_1 T_1 / (N_2 T_2)}{1 + N_1 / N_2} \right] \right\} \tau, \quad (16)$$

where

$$\tau \equiv \frac{k_B T_2}{0.55 \Lambda(T_2)(N_2/V_2)}. \quad (17)$$

Fig. 8 shows t_c as a function of bubble mass fraction N_1/N_2 for $T_1 = 10T_2$, $T_3 = T_2/10$ with $N_2/V_2 = 0.02 \text{ cm}^{-3}$ and $T_2 = 3 \times 10^7 \text{ K}$ as numbers typical of the central part of Hydra A (D2001). A bubble mass fraction ~ 1 percent yields cooling times of the expected order, 200 Myr.

4 DISTRIBUTION OVER T_{MIN}

In data taken with *Chandra* and *XMM/Newton* it is found that the plasma in any given cluster is confined to temperatures $T_{\text{max}} > T > T_{\text{min}}$, where typically $T_{\text{min}} > 10^7 \text{ K}$ (e.g. Böhringer et al. 2002, and references therein). In terms of the model discussed here, T_{max} and T_{min} are the largest and smallest temperatures at which there is significant emission measure. We now assume that the evolutionary time t of clusters is uniformly distributed in the interval $(0, t_{\text{cool}})$, where t_{cool} is the time required for the central temperature of a freshly reheated cluster to cool to zero. With this assumption and the approximation that we can neglect the evolution in the comoving density of clusters, we can calculate the fraction of observed clusters for which T_{min} lies in the range $(T + dt, T)$. We assume that the clusters are drawn at random from a flux-limited catalogue that was compiled with an instrument of limited spatial resolution. Hence, we focus exclusively on the total flux coming from plasma at a given temperature, and ignore issues related to the spatial distribution of the emission. This simplification is probably fairly realistic for current data.

First we determine the emission measure distribution of our model as shown in Fig. 7. Multiplying $E(t, T)$ by the cooling function $\Lambda(T)$ and integrating over T we obtain the cluster's bolometric luminosity $L(t)$. Dividing L by $4\pi D(z)^2$, where $D(z)$ is the luminosity distance of an object at redshift z (Carroll et al. 1992), we obtain the flux $S(z, t)$ of a cluster observed at evolutionary stage t :

$$S(z, t) = \frac{1}{4\pi D(z)^2} \int_0^\infty dt \Lambda(T) E(t, T). \quad (18)$$

We are interested in the number of clusters with $S > S_{\text{min}}$, so we invert this relation to find the redshift $z_{\text{max}}(t)$ out to which the cluster has $S > S_{\text{min}}$ at stage t . With our assumptions, the number of clusters detected at evolutionary stages in $(t + dt, t)$ is proportional to $V[z_{\text{max}}(t)] dt$, where $V(z)$ is the comoving volume to redshift z .

Similarly, the flux from plasma cooler than T_{min} in a cluster at redshift z is

$$S(T_{\text{min}}, z, t) = \frac{1}{4\pi D(z)^2} \int_0^{T_{\text{min}}} dt \Lambda(T) E(t, T), \quad (19)$$

which on inversion yields the maximum redshift $\hat{z}_{\text{max}}(T_{\text{min}}, t)$ out to which the cool plasma can be detected. Finally, the fraction of observed clusters in which plasma cooler than T_{min} can be detected is

$$f(T_{\text{min}}) = \frac{\int_0^{t_{\text{cool}}} dt V[\hat{z}_{\text{max}}(T_{\text{min}}, t)]}{\int_0^{t_{\text{cool}}} dt V[z_{\text{max}}(t)]}. \quad (20)$$

The lower two curves in Fig. 9 show $f(T_{\text{min}})$ for two

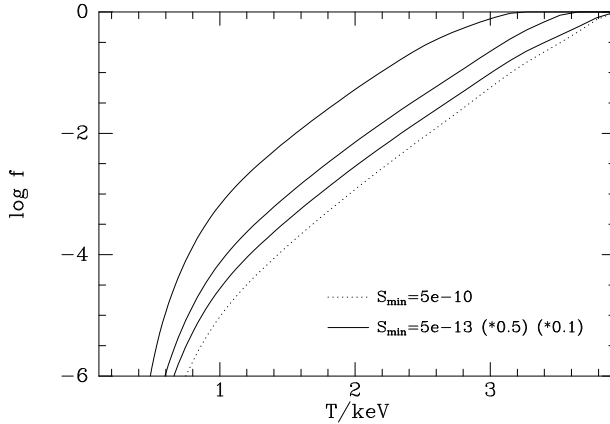


Figure 9. The fraction of detected clusters in which plasma cooler than T can be detected for two flux limits: $S_{\min} = 5 \times 10^{-10} \text{ erg cm}^{-2} \text{ s}^{-1}$ (dotted curve) and $S_{\min} = 5 \times 10^{-13} \text{ erg cm}^{-2} \text{ s}^{-1}$ (bottom full curve). The top full curve shows the fraction of clusters in the fainter sample in which plasma cooler than T would be detected in a pointed observation ten times more sensitive.

values of the limiting flux S_{\min} , namely 5×10^{-10} and $5 \times 10^{-13} \text{ erg cm}^{-2} \text{ s}^{-1}$ (dotted). For values of S_{\min} smaller than about $10^{-11} \text{ erg cm}^{-2} \text{ s}^{-1}$ the distance to which even the warmest plasma in Hydra can be seen is not large cosmologically, and $f(T_{\min})$ becomes insensitive to S_{\min} . At lower flux limits, cosmological dimming becomes significant, especially for the warmest plasma, and the fraction of clusters in which cooler plasma can be detected rises slightly.

The lower two curves in Fig. 9 predict that only $\sim 10^{-3}$ of clusters with bolometric luminosity in excess of S_{\min} will have a flux in excess of S_{\min} from gas cooler than $T \sim 2 \text{ keV}$. In practice when we examine a catalogue of clusters discovered in a magnitude-limited survey, gas at $T < 2 \text{ keV}$ will have been detected in a fraction of clusters that exceeds 10^{-3} because many clusters in the catalogue will have been the subject of more sensitive pointed observations subsequent to their discovery in the original survey. To quantify this effect, the upper two full curves in Fig. 9 show the fraction of clusters in which gas at temperatures below T gives rise to a flux in excess of $0.5S_{\min}$ and $0.1S_{\min}$ (top curve). From these curves we see that if the pointed observations are ten times as sensitive as the survey limit, the fraction of clusters showing gas at $T < 2 \text{ keV}$ rises to 5.6 percent, while the fraction showing gas at $T < 1 \text{ keV}$ is still only 0.04 percent.

5 DISTRIBUTION OVER σ_0

Kaiser (1991) pointed out that there is a gross discrepancy between the predictions of gravity-driven hierarchical models of structure formation and the statistics of X-ray astronomy. In particular, the theory of hierarchical structure formation predicts that the comoving density of X-ray sources was much higher at redshifts $z \gtrsim 1$ than is observed, and the cluster mass–X-ray luminosity relation is less steep than that observed. Kaiser pointed out that these conflicts would be eliminated if structure-formation theory were extended to include heating of the intergalactic medium (IGM) by massive stars and AGN prior to and at the epoch of

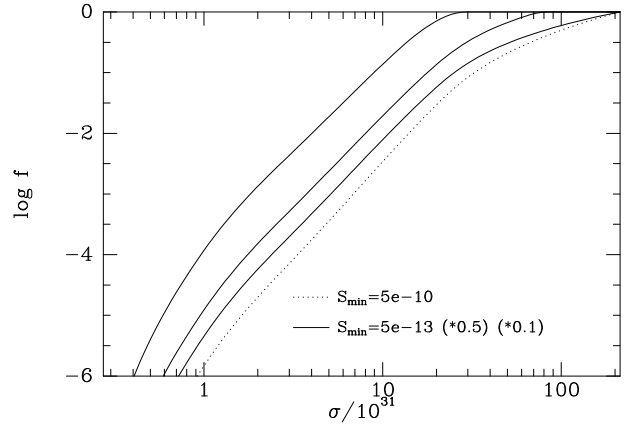


Figure 10. As Fig. 9 but giving the fractions of clusters in which plasma with entropy index smaller than σ would be detectable. The units of σ are as in Fig. 1. In these units $\sigma = 0.982k_B T n_e^{-2/3}$ with T in keV and n_e in cm^{-3} .

galaxy formation. As Kaiser pointed out, one should think of such heating as raising the adiabat on which the IGM lies. Lloyd-Davies et al. (2000) have attempted to determine the adiabat of the IGM by measuring the entropy index σ in galaxy groups and clusters at a distance of 10 percent of each system's virial radius, well outside the region in which radiative cooling is important. They define an entropy index $s = k_B T / n_e^{2/3}$ with units of keV cm^2 . Since $n/n_e = 21/11$, the conversion to our definition of σ is $1 \text{ keV cm}^2 = 9.82 \times 10^{30} \text{ cm}^4 \text{ g}^{-2/3} \text{ s}^{-2}$. Their 'entropy floor' of $s_{0.1} \sim 100 \text{ keV cm}^2$ is equal to the entropy index of gas at a radius of 200 kpc in our model of the Hydra cluster. This distance from the cluster centre corresponds to 10 percent of the virial radius of Hydra. The agreement is not surprising considering that the Hydra cluster was included in the study of Lloyd-Davies et al. (2000).

Lloyd-Davies et al. specifically excluded from consideration gas which they considered dense enough to have cooled significantly because they wished to probe the state of the IGM before clusters formed. In the context of our model of a cooling flow, it is interesting to ask whether they would have encountered an effective entropy floor even if they had not excluded cooling gas and had simply measured σ_0 , the minimum entropy index at the cluster centre. In Fig. 10 we show the fraction of clusters that have detectable emission from plasma with entropy index lower than σ – the calculation of this fraction proceeds in close analogy with that of Section 4. We see that in a pointed observation ten times more sensitive than the survey from which the targets were selected, only 1 percent of clusters would have detectable emission from plasma with $\sigma < 2 \times 10^{31} \text{ cm}^4 \text{ g}^{-2/3} \text{ s}^{-2} \approx 2 \text{ keV cm}^2$. Thus an 'entropy floor' with regard to the minimum entropy index of gas in galaxy clusters should be detectable in X-ray observations of clusters that have sufficient spatial resolution. This entropy floor is considerably lower than that found by Lloyd-Davies et al. (2000). It is determined by the very rapid cooling of the central regions of clusters, rather than any pre-heating of the gas before the collapse of the cluster that may explain the entropy floor at larger radii (Voit & Bryan 2001; McCarthy et al. 2002).

Since the systems discussed by Lloyd-Davies et al.

(2000) all contain galaxies, gas in these systems *did* cool at one time, so there must once have been gas on lower adiabats than that of the Lloyd-Davies et al. floor, $s_{0.1}$. It follows that gas was heated to $s \gtrsim s_{0.1}$ during or after the period of galaxy formation, and it is perfectly possible that the heating process involved nuclear outbursts of the type discussed here. In this case we have $s_{0.1} > \sigma_0^{\max}$, where σ_0^{\max} is the value taken by σ_0 immediately after an outburst: this inequality follows because Lloyd-Davies et al. find gas at $s_{0.1}$ that cannot cool, whereas now massive clusters still contain gas that can cool.

6 DISCUSSION

In the Hydra cluster we find that the distribution of mass in entropy index σ has a simple power-law form. We find that this form is to a good approximation preserved when the cluster gas cools in hydrostatic equilibrium. Thus the discovery that $M(\sigma)$ for Hydra fits a power law is no accident, but would have been discovered if we observed Hydra at an earlier or a later epoch.

We find that the central value of the entropy index, σ_0 , is a linear function of time until right up to the final cooling catastrophe that provokes an outburst of the central galactic nucleus. These results enable one to calculate the dynamics of a cooling flow with remarkable ease.

We estimate that in the absence of heat sources Hydra has about 280 Myr to run before there is a central cooling catastrophe. This result places a lower bound on the time between nuclear outbursts. The actual inter-outburst time is likely to be longer both because there is residual heating by supernovae/galactic winds and a low-level AGN, and because we have no reason to suppose that Hydra is in its immediate post-outburst state; it has probably been cooling for some time.

In trying to understand a cooling flow it is useful to focus on the system's entropy at least as much as on its energy. Between outbursts the story as regards entropy is simple: it is being radiated at a rate that can be readily calculated from the X-ray brightness profile. The story regarding energy is much more complicated: the gas losses energy radiatively but recovers some through the work done by both the surrounding IGM and the intracluster gravitational field. Our premise is that the nuclear outburst that is provoked by each cooling catastrophe restores the cluster gas to essentially the same state that it had immediately after the previous outburst. This premise requires that the entropy created by irreversible processes during each outburst is equal to the entropy radiated between outbursts.

We assume that the restructuring of the cluster gas during an outburst is effected by bubbles of plasma. We calculate both the entropy created when a bubble is inflated, and that created as it mixes in with, and heats, the bulk of the intracluster gas. The relative sizes of these two entropy sources is a weak function of the mass fraction that passes through bubbles during an outburst, but is typically of order 3–5. If a few percent of the cluster gas passes through bubbles during an outburst, the time between outbursts is a few hundred Myr, as the observations suggest.

When gas cools from temperatures $\gtrsim 3$ keV at which bremsstrahlung is the dominant cooling process, it spends

only a very small fraction of the total cooling time at $T < 1$ keV. In the case of cluster gas this effect is magnified by the large density contrast between the cluster centre and the half-mass radius. Consequently, not only does gas at $T < 1$ keV exist only for a very small fraction of the inter-outburst time, but it is confined to an extremely small fraction of the total volume. We have used our simple models of cooling flows to calculate the fraction of clusters in a magnitude-limited sample in which gas cooler than temperature T would be detectable. We find that without pointed observations gas cooler than 2 keV would be found in only $\sim 10^{-3}$ of clusters; with pointed observations ten times more sensitive than the discovery survey, such cool gas would be detected in ~ 4 percent of clusters. Thus, we should not be surprised to find that gas cooler than ~ 1 keV has not been detected in clusters observed by *XMM* and *Chandra*.

Similarly, we predict that pointed observations of a complete sample of clusters would detect gas at entropies below $\sigma \sim 2$ keV cm² in only ~ 1 percent of clusters because low-entropy gas appears only fleetingly and in small volumes. This lower limit on the entropy is at a value of σ that is a factor ~ 50 lower than the ‘entropy floor’ claimed for intergalactic gas from X-rays studies of low-mass clusters at radii well outside the region where radiative cooling is important. However, with the spectral and spatial resolution of *XMM* and *Chandra* the lower entropy limit should be detectable in samples of galaxy clusters.

ACKNOWLEDGMENTS

We are grateful to L.P. David for supplying data for the Hydra cluster in digital form.

REFERENCES

- Binney J., Tabor G., 1995, MNRAS, 276, 663
- Binney J. J., 1996, in Proceedings of the 36th Herstmonceux conference. Cambridge University Press, p. 89
- Binney J. J., 1999, in Röser H.-J., Meisenheimer K., eds, The radio galaxy Messier 87. Springer, p. 116
- Binney J. J., 2002, in Laing R. A., Blundell K. M., eds, Particles and fields in radio galaxies. ASP Conference Series
- Binney J. J., Tremaine S., 1987, Galactic Dynamics. Princeton University Press
- Böhringer H., Matsushita K., Churazov E., Ikebe Y., Chen Y., 2002, A&A, 382, 804
- Brüggen M., Kaiser C. R., 2001, MNRAS, 325, 676
- Brüggen M., Kaiser C. R., Churazov E., Enßlin T. A., 2002, MNRAS, 331, 545
- Carroll S. M., Press W. H., Turner E. L., 1992, ARA&A, 30, 499
- Churazov E., Brüggen M., Kaiser C. R., Böhringer H., Forman W., 2001, ApJ, 554, 261
- Ciotti L., Ostriker J. P., 1997, ApJ, 487, L105
- Ciotti L., Ostriker J. P., 2001, ApJ, 551, 131
- David L. P., Nulsen P. E. J., McNamara B. R., Forman W., Jones C., Ponman T., Robertson B., Wise M., 2001, ApJ, 557, 546, [D2001]
- Fabian A. C., 1994, ARA&A, 32, 277

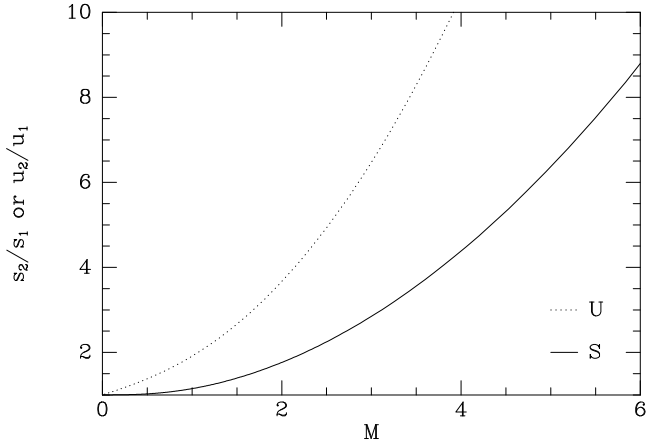


Figure 11. Entropy change across a shock.

Fabian A. C., Sanders J. S., Ettori S., Taylor G. B., Allen S. W., Crawford C. S., Iwasawa K., Johnstone R. M., Ogle P. M., 2000, MNRAS, 318, L65
 Heinz S., Reynolds C. S., Begelman M. C., 1998, ApJ, 501, 126
 Kaiser C. R., Alexander P., 1999, MNRAS, 305, 707
 Kaiser N., 1991, ApJ, 383, 104
 Lloyd-Davies E. J., Ponman T. J., Cannon D. B., 2000, MNRAS, 315, 689
 McCarthy I. G., Babul A., Balogh M. L., 2002, ApJ, 573, 515
 Navarro J. F., Frenk C. S., White S. D., 1996, ApJ, 462, 563
 Quilis V., Bower R. G., Balogh M. L., 2001, MNRAS, 328, 1091
 Saxton C. J., Sutherland R. S., Bicknell G. V., 2001, ApJ, 563, 103
 Tabor G., Binney J. J., 1993, MNRAS, 263, 323
 Voit G. M., Bryan G. L., 2001, Nat., 414, 425

APPENDIX: ENTROPY GENERATION IN SHOCKS

A major source of entropy production is shock fronts. Consider a perpendicular shock front in which an ideal monatomic gas with specific entropy s_1 , specific internal energy u_1 and speed v_1 is converted into material in which the same quantities are denoted s_2 , u_2 and v_2 . Then conservation of mass, momentum and energy across the shock front yield

$$\frac{s_1}{s_2} = \frac{r_1}{r_2} \left(\frac{5r_2/3 + 1/2}{5r_1/3 + 1/2} \right), \quad (21)$$

where the $r_i \equiv u_i/v_i^2$ are the two roots of the quadratic equation

$$\frac{(2r/3 + 1)^2}{5r/3 + 1/2} = \text{constant}. \quad (22)$$

Fig. 11 shows the changes in u and s across a shock front as a function of the Mach number¹ of the shock, $M =$

$(v_1 - v_2)/c_s$. The very slow rise of the curve for s_2/s_1 at small values of M implies that weak shocks are very ineffective entropy generators. The much steeper rise in the curve for u_2/u_1 shows that weak shocks do thermalize energy effectively, but since they do so without significant entropy increase, the original bulk kinetic energy can be largely recovered by subsequent adiabatic expansion.

¹ Our definition of M differs significantly from a common one that involves the upstream speed relative to the shock. With our

definition, in the limit of a sound wave $M \rightarrow 0$, rather than $M \rightarrow 1$ as in the case of the alternative definition.